

# Stochastic Evolution of Pancreatic Cancer Metastases During Logistic Clonal Expansion

Kimiyo N. Yamamoto, MD, PhD<sup>1,2,3,4</sup>; Lin L. Liu, PhD<sup>1,2</sup>; Akira Nakamura, MD, PhD<sup>5</sup>; Hiroshi Haeno, PhD<sup>6</sup>; and Franziska Michor, PhD<sup>1,2,3,7,8</sup>

Despite recent progress in diagnostic and multimodal treatment approaches, most cancer deaths are still caused by metastatic spread and the subsequent growth of tumor cells in sites distant from the primary organ. So far, few quantitative studies are available that allow for the estimation of metastatic parameters and the evaluation of alternative treatment strategies. Most computational studies have focused on situations in which the tumor cell population expands exponentially over time; however, tumors may eventually be subject to resource and space limitations so that their growth patterns deviate from exponential growth to adhere to density-dependent growth models. In this study, we developed a stochastic evolutionary model of cancer progression that considers alterations in metastasis-related genes and intercellular growth competition leading to density effects described by logistic growth. Using this stochastic model, we derived analytical approximations for the time between the initiation of tumorigenesis and diagnosis, the expected number of metastatic sites, the total number of metastatic cells, the size of the primary tumor, and survival. Furthermore, we investigated the effects of drug administration and surgical resection on these quantities and predicted outcomes for different treatment regimens. Parameter values used in the analysis were estimated from data obtained from a pancreatic cancer rapid autopsy program. Our theoretical approach allows for flexible modeling of metastatic progression dynamics.

Clin Cancer Inform. © 2019 by American Society of Clinical Oncology

Licensed under the Creative Commons Attribution 4.0 License 

## INTRODUCTION

Metastasis is the major cause of death of patients with cancer. Metastatic disease is often observed at the time of detection of the primary tumor, although its frequency varies among cancer types. Up to 60% of lung and pancreatic cancers and approximately 20% of breast, prostate, and bladder cancers are metastatic at diagnosis.<sup>1</sup> Even for apparently nonmetastatic disease upon diagnosis, undetectable micrometastases often result in treatment failure. This finding is consistent with the fact that circulating tumor cells, which have the potential to lead to metastatic lesions, are present in patients diagnosed with early-stage disease.<sup>2</sup> Therefore, an accurate evaluation of the chance of metastatic disease at a particular stage of tumorigenesis, such as at diagnosis and treatment initiation, is of clinical importance.

The metastatic process consists of several steps,<sup>3</sup> many of which are governed by the conversion between two cellular states—the epithelial and mesenchymal phenotypes. Epithelial–mesenchymal transition (EMT) is a key regulatory program that plays an essential role in promoting tumor invasion and metastasis in epithelium-derived carcinomas.<sup>4</sup> The EMT

process is driven by the upregulation of core groups of transcriptional regulators, such as the Snail zinc-finger family.<sup>5-7</sup> In contrast to the upregulation of EMT-related genes, inactivation of specific regions of the genome, such as NM23,<sup>8,9</sup> also promotes metastatic formation in various cancer types. Alterations in these genes serve as examples for situations in which a single genetic change is sufficient to confer metastatic potential to cancer cells. After the dissemination of tumor cells from the primary site, a mesenchymal-epithelial transition often occurs, which allows tumor cells to reinitiate growth at the metastatic site.<sup>10</sup>

A number of mathematical modeling methods have been designed to understand tumor dynamics and metastasis formation.<sup>11,12</sup> In the 1980s, a logistic regression model was used to predict outcomes of patients with metastatic testicular cancer.<sup>13</sup> Later on, a model of competition between tumor and normal cells during chemotherapy was described that also considered the presence of metastatic cells.<sup>14</sup> How a delay of surgery increases the risk of metastases in patients with breast cancer was also investigated.<sup>15</sup> The dynamic interactions between the primary tumor and metastases were also studied for situations in which metastases arise early from the primary tumor.<sup>16</sup>

## ASSOCIATED CONTENT

### Data Supplement

Author affiliations and support information (if applicable) appear at the end of this article.

### Accepted on

December 12, 2018

and published at

[ascopubs.org/journal/](https://ascopubs.org/journal/cci)

[cci](https://doi.org/10.1200/CCI.18.00079) on March 22,

2019: DOI [https://doi.](https://doi.org/10.1200/CCI.18.00079)

[org/10.1200/CCI.18.](https://doi.org/10.1200/CCI.18.00079)

00079

Branching process models were used to investigate the dynamics of metastasis formation.<sup>17-21</sup> Several modeling contributions to studying metastasis have been made by incorporating tumor-microenvironment interactions, including the effect of the extracellular matrix<sup>22</sup> and lymphatic and blood systems.<sup>23,24</sup> Another approach also considered network relationships among different organs within a directed graphical model framework. This method directly estimated tumor migration rates from organ to organ using large autopsy data sets of patients with metastases.<sup>25,26</sup>

An important aspect of mathematical modeling of tumor growth is the choice of the appropriate growth kinetic model. Different aspects of tumor growth kinetics have been extensively investigated, both experimentally and theoretically, for more than half a century.<sup>27-35</sup> Exponential growth is the simplest assumption used in tumor growth models. In such a model, cancer cells proliferate with a cell-cycle duration independent of the total tumor size.<sup>27</sup> This model potentially represents an accurate functional form that describes early tumor growth; however, a more general class of models (eg, an increasing curve asymptotically converging to a maximum size [ie, a carrying capacity]) may be more appropriate for describing long-term growth of solid tumors subject to the limited availability of nutrients, oxygen, and space. In several investigations, empirically observed tumor growth kinetics were well described by logistic or Gompertz models.<sup>30-36</sup> Previous mathematical frameworks for investigating tumor progression and metastasis formation, however, mostly relied on an exponential growth model. In contrast, in this work we designed and analyzed a three-step logistic stochastic model of the evolution of metastasis caused by an epigenetic alteration in an expanding population of pancreatic cancer cells. Our study represents a departure from existing stochastic models of metastasis formation as we incorporated mechanisms of feedback inhibition to achieve a decreasing growth rate with an asymptotically limiting total size, thereby obtaining a potentially more realistic description of the evolutionary dynamics of the system. We then used this mathematical model to derive analytical approximations of several quantities of interest, including the time between the initiation of tumorigenesis and diagnosis, the expected number of metastatic sites, the total number of metastatic cells, the size of the primary tumor, and survival. We also used the model to evaluate the effects of alternative treatment strategies *in silico* using the stochastic logistic model.

## RESULTS

### Logistic Stochastic Model for Pancreatic Cancer Progression and Metastasis

Our model considers a stochastic logistic branching process that starts from a single cell in the primary site. The initiating population has not yet evolved the potential to disseminate and consists entirely of so-called type-0 cells.

During each division event of a type-0 cell, with probability  $u$ , a cell might arise that has evolved metastatic potential but that still resides in the primary tumor. Such a cell is called a type-1 cell. The growth rate of the entire tumor is given by an increasing curve with an inflection point that asymptotically converges to a maximal number, the carrying capacity (Fig 1). Within this stochastic model, the numbers of type-0 and type-1 cells at time  $t$  are denoted by  $x_0$  and  $x_1$ , respectively. When the number of type-0 and type-1 cells at time  $t$  are  $x_0 = k_0$  and  $x_1 = k_1$ , type-0 cells divide at rate

$$r_0 \left( 1 - \frac{k_0 + k_1}{M_{\text{carryP}}} \right)$$

and die at rate  $d_0$  per unit time, where  $M_{\text{carryP}}$  denotes the carrying capacity of the primary site. Similarly, type-1 cells divide at rate

$$r_1 \left( 1 - \frac{k_0 + k_1}{M_{\text{carryP}}} \right)$$

and die at rate  $d_1$  per unit time. Type-1 cells can emigrate to a distant site and establish a metastatic site at rate  $q$  per unit time, where they are called type-2 cells. The number of cells at the  $i$ -th metastatic site is denoted by  $x_{2i}$ . When the number of cells at the  $i$ -th metastatic site is  $x_{2i} = k_{2i}$ , type-2 cells at that site divide at rate

$$r_2 \left( 1 - \frac{k_{2i}}{M_{\text{carryM},i}} \right)$$

and die at rate  $d_2$  per unit time, where  $M_{\text{carryM},i}$  denotes the carrying capacity of the  $i$ -th metastatic site. Total numbers of tumor cells at diagnosis and death are denoted by  $M_{\text{diag}}$  and  $M_{\text{death}}$ , respectively (Fig 1B). A more detailed description of the model and notations can be found in the Data Supplement.

### Estimation of Parameters of the Stochastic Logistic Process From Clinical Data

To parameterize our model, we used a clinical database of 101 patients with pancreatic cancer who consented to an autopsy within the Gastrointestinal Cancer Rapid Medical Donation Program at Johns Hopkins University (Data Supplement).<sup>19,37</sup> For these patients, data on primary tumor size and metastatic burden at autopsy were recorded using computed tomography images. Median diameters of the primary and the largest metastasis at death were 5 cm (first and third quantile, 4 and 6 cm) and 2.5 cm (first and third quantile, 1.5 and 3.5 cm), respectively (Data Supplement). On the basis of this database, we set the carrying capacity of the logistic stochastic process as the median of the measured sizes of primary tumors at death. To consider the diversity in sizes of metastases within one patient, carrying capacities for metastatic sites were obtained from a normal distribution with a mean and variance estimated from the

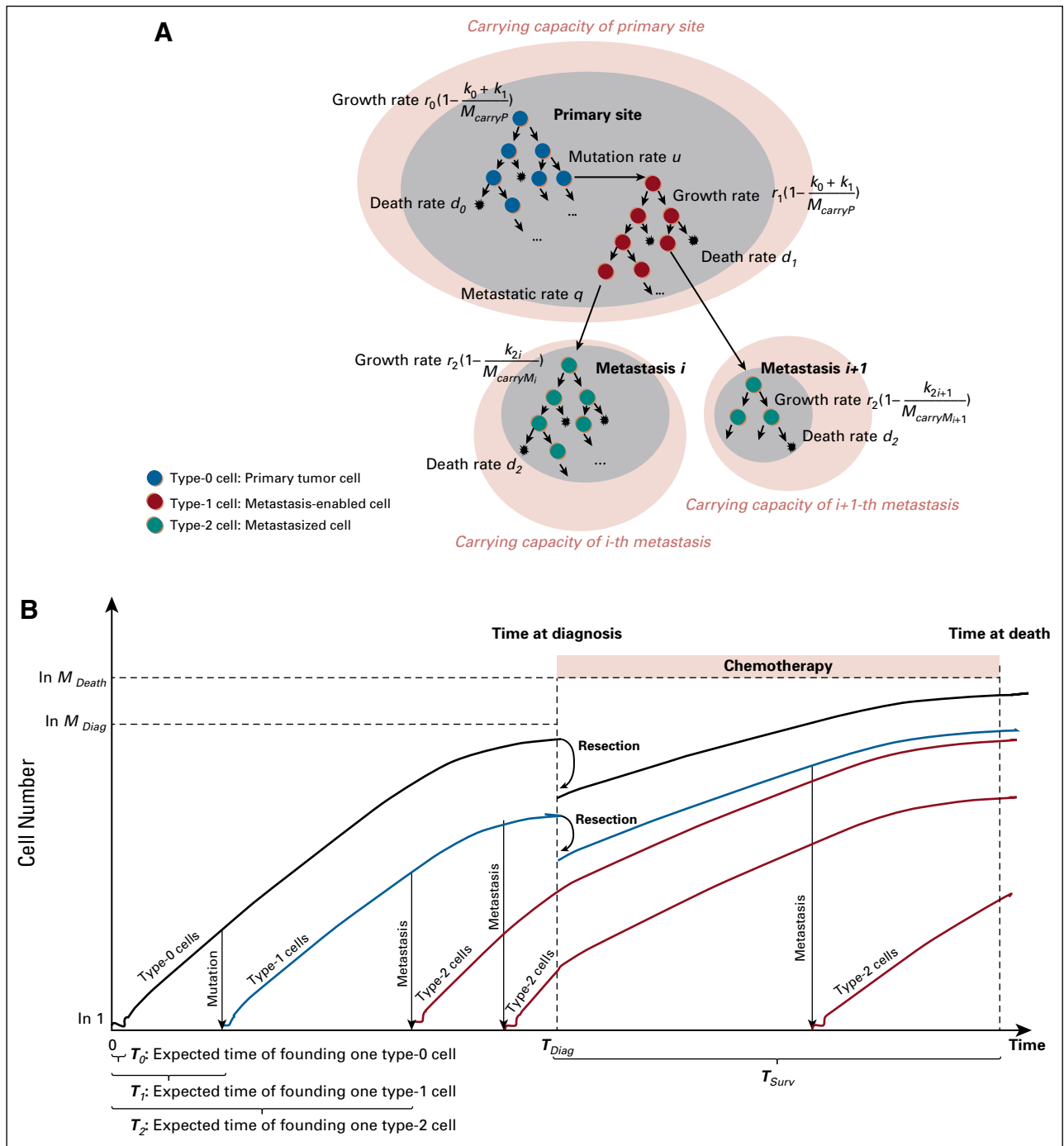


**FIG 1.** Schematic illustration of the model. (A) Mathematical framework and (B) a schematic illustration of the model. We considered stochastic expansion of a tumor cell population starting from a single cell in the primary site. In our model, tumor growth rate decreases with increasing tumor size—that is, it is given by an increasing curve with an inflection point that asymptotically converges to a maximal number, the carrying capacity. Cells that have not yet evolved the ability to metastasize, type-0 cells, divide and die at rates  $r_0(1 - \frac{k_0 + k_1}{M_{carryP}})$  and  $d_0$  when the number of type-0 and type-1 cells are  $x_0 = k_0$  and  $x_1 = k_1$  at time  $t$ . Type-0 cells give rise to type-1 cells with probability  $u$  per type-0 cell division. Type-1 cells divide and die at rates  $r_1(1 - \frac{k_0 + k_1}{M_{carryP}})$  and  $d_1$ . Type-1 cells can establish a type-2 cell with probability  $q$  per time unit. When the number of cells at the  $i$ -th metastatic site is  $x_{2i} = k_{2i}$ , type-2 cells at that site divide and die at rates  $r_2(1 - \frac{k_{2i}}{M_{carryM_i}})$  and  $d_2$ . When the total number of all tumor cells reaches  $M_{diag}$ , the tumor is detected and treatment in the form of chemotherapy and/or surgery initiates. Surgery reduces the number of cells at the primary site by  $1 - \epsilon$ , and chemotherapy reduces the growth rate or increases the death date of all cells by a factor of  $\gamma$  and  $\eta$ , respectively. When the total number of cells reaches  $M_{death}$ , a patient dies. Diag, diagnosis; Surv, survival.

database (Data Supplement) as 2.5 and 5.3 cm, respectively. Other parameter values of the stochastic model were obtained from previous studies.<sup>19,37,38</sup> For each parameter set, we performed a large number of computer simulations to obtain data on the mean and variance of each quantity, such as the probability of metastases at diagnosis and the number of metastatic sites at death.

### Analytical Approximations of the Primary Cell Number and Time Until Diagnosis

As large-scale stochastic simulations are computationally expensive, we sought to derive analytical approximations that provide closed-form solutions and can be used to quickly predict quantities of interest of the stochastic process. Such approximations are often derived in the field of stochastic mathematical modeling because simulations of the stochastic process are inefficient to address such questions as optimum treatment schedules or computationally expensive searches through large ranges of parameters.<sup>20,21,39</sup> The Data Supplement provides notations used for these analytical approximations. For all analytical calculations, we only considered a deterministic approximation to the mean behavior of the stochastic process and did not aim to predict the variance or other moments of the process; these quantities are the topic of future investigations. We then confirmed the accuracy of the approximations using simulation results of the logistic stochastic process model.

We first aimed to derive a set of logistic differential equations to describe the changes in cell numbers over time. Within the deterministic approximation, let the numbers of type-0, type-1, and type-2 cells at time  $t$  be denoted by  $X_0(t)$ ,  $X_1(t)$  and  $X_2(t)$ . Here, we assumed that type-0 cells first appeared at time  $T_0$ , a type-1 lineage was first generated at time  $T_1$ , and a type-2 lineage first emerged at time  $T_2$ . The cell numbers are then given as followings:

$$X_0(t) = \frac{M_0}{1 + (M_0 - 1)e^{-(r_0 - d_0)(t - T_0)}} \quad (1)$$

$$X_1(t) = \frac{M_1}{1 + (M_1 - 1)e^{-(r_1 - d_1)(t - T_1)}} \quad (2)$$

$$X_2(t) = \frac{M_{carryM}}{1 + (M_{carryM} - 1)e^{-(r_2 - d_2)(t - T_2)}} \quad (3)$$

The Data Supplement provides details of the derivation. The quantities  $M_0$  and  $M_1$  represent the carrying capacities of type-0 and type-1 cells, respectively, in the primary site.  $T_0$ ,  $T_1$ , and  $T_2$  represent the times at which the expected numbers of type-0, type-1, and type-2 cells, respectively, are 1. The Data Supplement provides details of the derivations of  $M_0$  and  $M_1$ , as well as for  $T_0$ ,  $T_1$ , and  $T_2$ . The

quantity  $M_{carryM}$  represents the carrying capacity of type-2 cells, which is estimated  $M_{carryM}$  from our clinical database.<sup>19,37</sup> We next defined  $T_{diag}$  as time from the initiation of tumorigenesis to diagnosis (Data Supplement). This expression is given by

$$T_{diag} := \inf\{t : X_0(t) + X_1(t) + X_2(t) = M_{diag}\} \quad (4)$$

In words, we defined the time of tumor diagnosis as the time at which the sum of the number of type-0, -1, and -2 cells is equal to  $M_{diag}$ , the number of tumor cells at diagnosis. The quantity  $M_{diag}$  was again estimated from the clinical database.<sup>19,37</sup>

We then investigated the accuracy of Equations 1 and 2 using exact computer simulations of the stochastic logistic process for a wide range of parameter values. To evaluate Equations 1 and 2 at the time of diagnosis, we substituted  $T_{diag}$  for the expression of time  $t$  in these equations (Data Supplement). We found that the analytical approximations accurately predicted the simulation results (Data Supplement). We observed that an increase in the growth rates of primary cells, tumor size at diagnosis  $M_{diag}$ , and the carrying capacity of the primary site  $M_{carryP}$  resulted in an increase in the number of type-0 cells (Data Supplement), whereas an increase in the (epi)genetic alteration rate  $u$ , as well as  $M_{diag}$  and  $M_{carryP}$ , resulted in an increase in the number of type-1 cells (Data Supplement). We then investigated the accuracy of Equation 4 compared with exact simulations of the stochastic logistic process (Fig 2). When doing so, we found that Equation 4 accurately predicted our simulation results. We observed that an increase in growth rates of primary cells and  $M_{carryP}$  decreased the time from the initiation of tumorigenesis until detection, whereas an increase in death rates of primary cells and  $M_{diag}$  led to an increase in the time until detection (Figs 2C-2F). However, increases in  $u$ ,  $q$ , and  $M_{carryM}$  did not affect the time until detection (Figs 2A, 2B, and 2G).

### Analytical Approximations of Metastatic Properties at Diagnosis

We then aimed to derive analytical approximations of quantities of interest related to metastatic sites. We first derived the expected number of metastatic sites at diagnosis, denoted as  $L_{diag}$  (Fig 3 and Data Supplement). When considering all metastatic events between the first emergence of type-1 cells and diagnosis, we determined  $L_{diag}$  to be given by

$$L_{diag} := \int_{T_1}^{T_{diag}} qX_1(t)dt \quad (5)$$

where  $X_1(t)$  can be evaluated using Equation 2.

When comparing the predictions of Equation 5 to exact simulations of the stochastic logistic process, we found that Equation 5 accurately predicted simulation results (Fig 3). We observed that an increase in  $u$ ,  $q$ , and  $M_{diag}$  resulted in

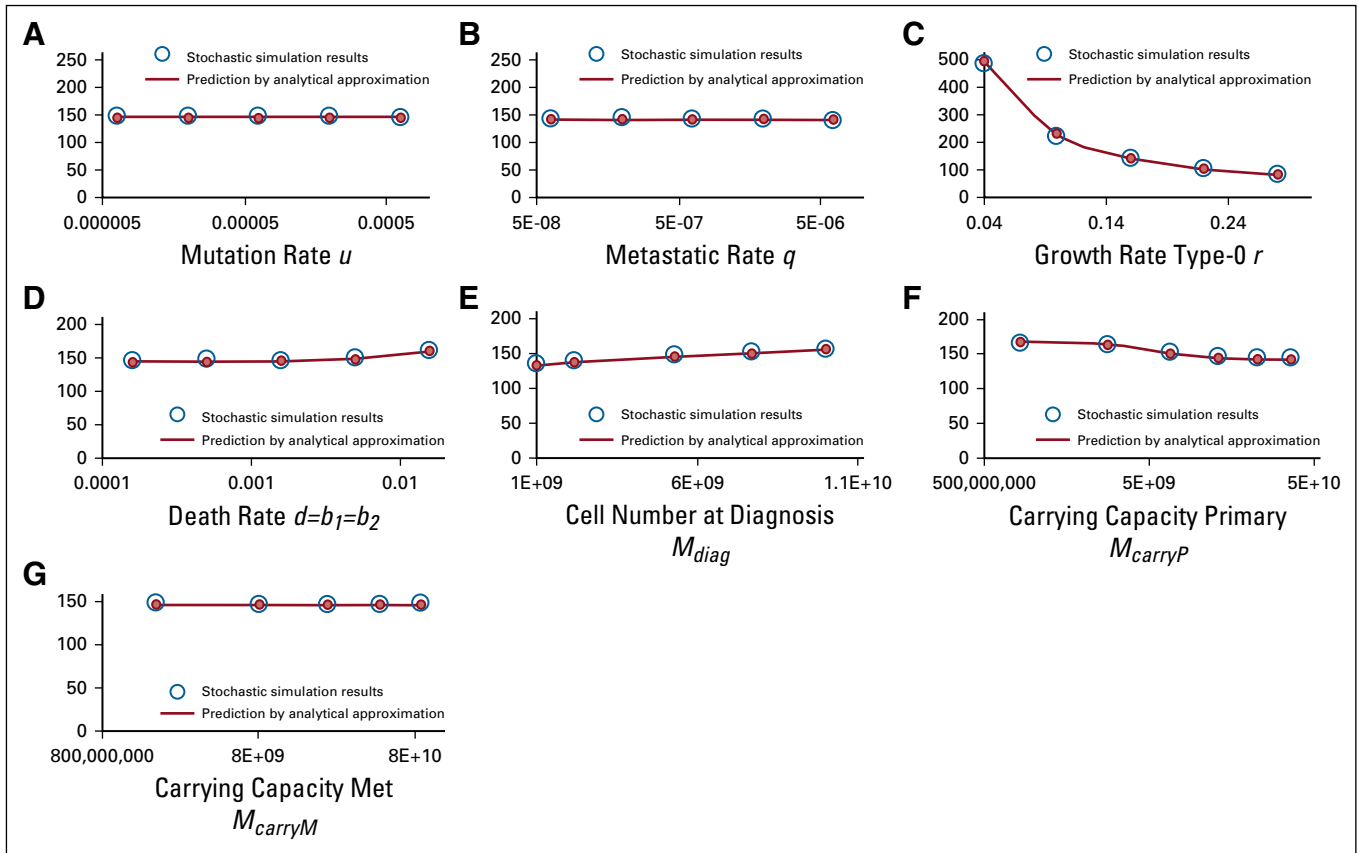


**FIG 2.** Time from the initiation of tumorigenesis to diagnosis (diag). Panels show the dependence of the time from the initiation of tumorigenesis to diagnosis on various parameters. The red curves indicate the predictions of the analytical approximation, Equation 4, and the circles indicate the results of computer simulations. Parameters estimated from data obtained from the rapid autopsy program<sup>37</sup>;  $r_0 = r_1 = 0.16$ ;  $r_2 = 0.58$ ;  $d_0 = d_1 = 0.0016$ ;  $d_2 = 0.0058$ ;  $M_{diag} = 5.3 \times 10^9$ ;  $u = 6.31 \times 10^{-5}$ ;  $q = 6.31 \times 10^{-7}$ ;  $M_{carryP} = 1.3 \times 10^{10}$ ;  $M_{carryM} = N(2.5, 5.3)$  cm in diameter. Met, metastatic.

an increase in the expected number of metastatic sites (Figs 3A, 3B, and 3E). We also found that the number of metastatic sites decreased when the growth rates of primary cells and  $M_{carryP}$  were small (Figs 3C and 3F). This effect may arise because the chance of a metastatic event decreases as a result of the small size of the primary tumor at diagnosis in this parameter region (Data Supplement). The number of metastatic sites also decreases when growth rates of primary cells and  $M_{carryP}$  are large (Figs 3C and 3F), likely as a result of the short time from tumor initiation until diagnosis (Figs 2C and 2F).

We next derived the expected number of metastatic cells at diagnosis (Fig 4 and Data Supplement). We defined  $P_{k_1}$  as the probability that a successful type-2 lineage arises when there are  $x_1 = k_1$  type-1 cells (Data Supplement). This quantity is given by

$$p_{k_1} = 1 - e^{-\frac{q}{1-d_1/r_1}}$$

on the basis of previous results.<sup>39</sup> We then defined  $Q_{k_1}$  as the number of type-2 cells at diagnosis conditioned on the event that the first type-2 cell arose when there were  $x_1 = k_1$

type-1 cells (Data Supplement). The quantity  $Q_{k_1}$  is given by

$$Q_{k_1} = \frac{M_{carryM}}{1 + (M_{carryM} - 1)e^{-(r_2 - d_2)(T_{diag} - T_1 - \tau(k_1))}} \quad (6)$$

Here,  $\tau(k_1)$  represents the amount of time between the first emergence of type-1 cells and when there are  $x_1 = k_1$  type-1 cells, which is given by

$$\tau(k_1) = \frac{\ln(k_1)}{r_1 - d_1}$$

The expected number of metastatic cells at diagnosis is then given by

$$\sum_{k_1=1}^{N_{type1,diag}} P_{k_1} Q_{k_1} \quad (7)$$

Here,  $N_{type1,diag}$  represents the number of type-1 cells at diagnosis. The Data Supplement provides details of the derivation.

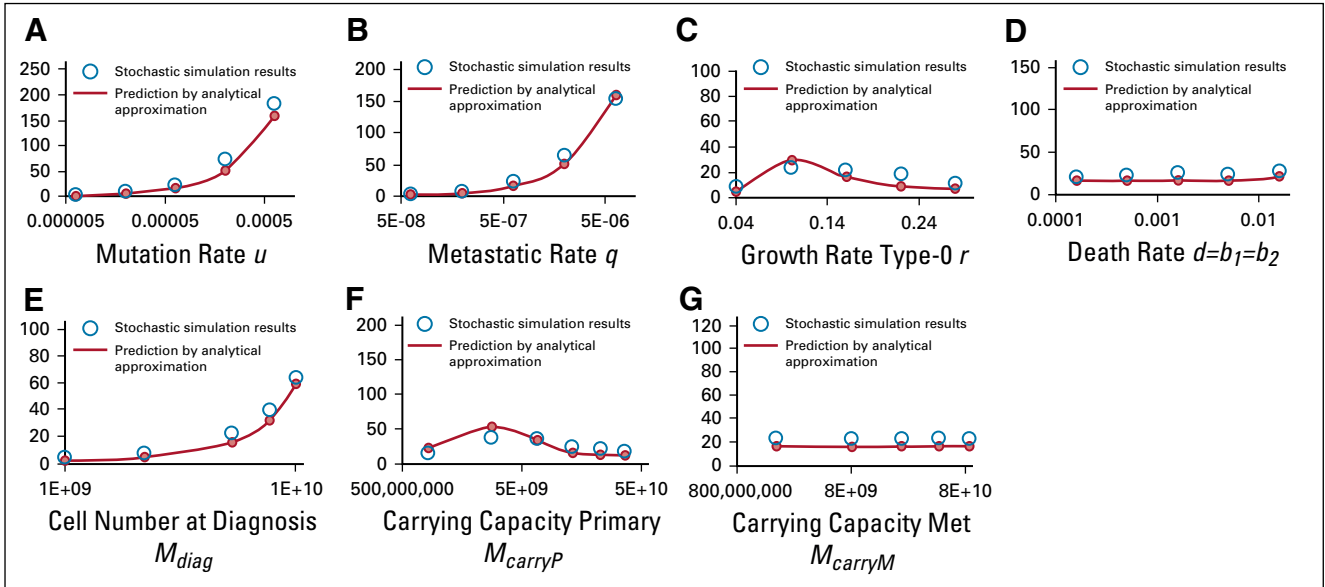


**FIG 3.** The number of metastatic (Met) sites at diagnosis (diag). Panels show the dependence of the number of metastatic sites on various parameters. The red curves indicate the predictions of the analytical approximation, Equation 5, and the circles indicate the results of computer simulations. Parameters are the same as described in Figure 2.

Again, we found that Equation 7 accurately predicts our simulations results (Fig 4). We observed that increases in  $u$ ,  $q$ ,  $M_{diag}$ , and  $M_{carryM}$  resulted in an increase in the number of metastatic cells (Figs 4A, 4B, 4E, and 4G). We found that the number of metastatic cells was large when the growth rates of primary cells and  $M_{carryP}$  were small (Figs 4C and 4F). This effect may arise because metastatic cells can preferentially emerge in situations of a more slowly growing primary tumor and/or a primary tumor with a limited carrying capacity.

### Analytical Approximation of Survival and Metastatic Properties at Death

We next considered tumor dynamics after diagnosis, including the option of chemotherapy to reduce the growth rates of tumor cells by a factor of  $\gamma$  and increase the death rates of all tumor cells by a factor of  $\eta$ , as well as surgical resection to reduce the number of primary cells by  $1 - \epsilon$ .

We defined  $T_{surv}$  as survival after diagnosis and derived an analytical approximation of this quantity (Data Supplement). We considered death to occur when the total number of type-0, type-1, and type-2 cells is equal to  $M_{death}$ , then  $T_{surv}$  is calculated as the solution to

$$T_{surv} = \inf \{ t : X_{0,chemo}(t) + X_{1,chemo}(t) + X_{2,chemo}(t) = M_{death} \} \quad (8)$$

where  $t$  is the unknown. Here,  $X_{0,chemo}(t)$ ,  $X_{1,chemo}(t)$ , and  $X_{2,chemo}(t)$  represent the number of cells of each type at

time  $t$  during chemotherapy. The Data Supplement provides detailed derivations. We defined  $L_{death}$  as the expected number of metastatic sites at death, given by

$$L_{death} = L_{diag} + \int_0^{T_{surv}} q X_{1,chemo}(t) dt \quad (9)$$

Finally, we derived an analytical approximation of the number of metastatic cells at death (Data Supplement). We first considered the number of type-2 cells generated before diagnosis. We defined  $\kappa(k_1)$  as the amount of time between the emergence of a type-2 cell generated when there were  $x_1 = k_1$  type-1 cells and diagnosis given that chemotherapy was administered starting from the emergence of the type-2 lineage (Data Supplement). This quantity is calculated as

$$\frac{M_{carryM}}{1 + (M_{carryM} - 1)e^{-(r_2' - d_2')\kappa(k_1)}} = Q_{k_1} \quad (10)$$

Of note,  $Q_{k_1}$  above represents the number of type-2 cells at diagnosis that were generated when there were  $x_1 = k_1$  type-1 cells, which was obtained from Equation 6. We then defined  $R_{k_1}$  as the cell number within a type-2 lineage at the time of death given that the type-2 lineage was generated from  $x_1 = k_1$  type-1 cells before diagnosis. The quantity  $R_{k_1}$  as

$$R_{k_1} = \frac{M_{carryM}}{1 + (M_{carryM} - 1)e^{-(r_2' - d_2')(T_{surv} + \kappa(k_1))}}$$

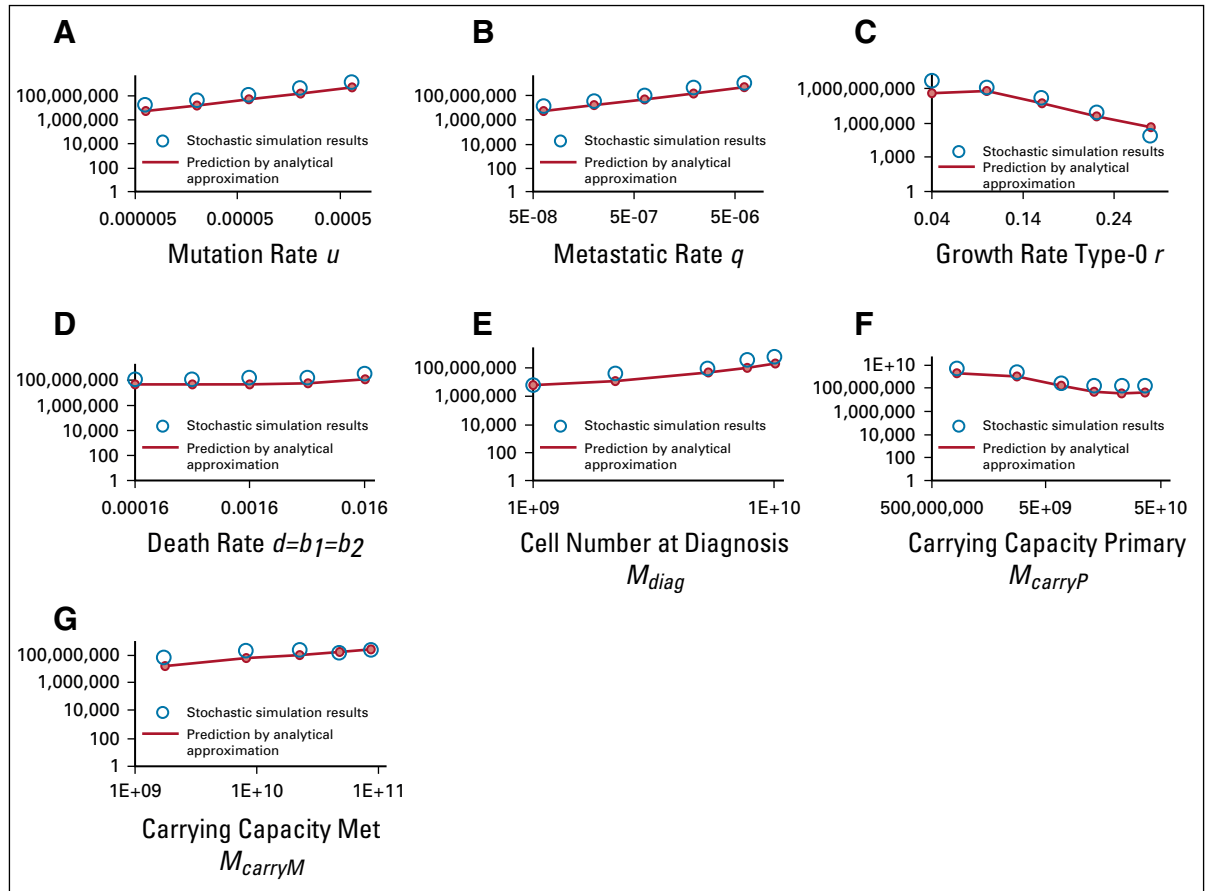


**FIG 4.** The number of metastatic (Met) cells at diagnosis (diag). Panels show the dependence of the number of metastatic cells on various parameters. The red curves indicate the predictions of the analytical approximation, Equation 7, and the circles indicate the results of computer simulations. Parameters are the same as described in Figure 2.

Then, the total number of type-2 cells at death, which were generated from type-1 cells before diagnosis, is given by

$$N_{type2death1} = \sum_{k_1=1}^{N_{type1diag}} P_{k_1} R_{k_1}$$

We next considered type-2 cells generated after diagnosis. We defined  $\sigma(k_1)$  as the amount of time between diagnosis and the time at which the number of type-1 cells reaches  $x_1 = k_1$  given that both surgical resection and chemotherapy were administered at diagnosis (Data Supplement). The quantity  $\sigma(k_1)$  is calculated as

$$\sigma(k_1) = \frac{\ln(k_1 / \varepsilon N_{type1diag})}{r_1' - d_1'}$$

We then defined  $S_{k_1}$  as the cell number of a type-2 lineage at death given that the type-2 lineage was generated from  $x_1 = k_1$  type-1 cells after diagnosis (Data Supplement). This quantity is given by

$$S_{k_1} = \frac{M_{carryM}}{1 + (M_{carryM} - 1)e^{-(r_2' - d_2')(T_{surv} - \sigma(k_1))}}$$

Then, the total number of type-2 cells at death, given that they were generated from type-1 cells after diagnosis, is given by

$$N_{type2death2} = \sum_{k_1=N_{type1diag}}^{N_{type1death}} P_{k_1} S_{k_1}$$

Finally, the expected number of metastatic cells at death is then given by

$$N_{type2death1} + N_{type2death2} = \sum_{k_1=1}^{N_{type1diag}} P_{k_1} R_{k_1} + \sum_{k_1=N_{type1diag}}^{N_{type1death}} P_{k_1} S_{k_1} \quad (11)$$

Here,  $N_{type1death}$  represents the number of type-1 cells at death (see the Data Supplement for details of this derivation).

We then again sought to validate these approximate quantities using exact computer simulations of the stochastic logistic process. We found that Equations 8, 9, and 11 in the main text as well as in the Data Supplement

accurately predict the simulation results (Fig 5 and Data Supplement). We observed that an increasing effect of chemotherapies—that is, increasing  $\gamma$  and  $\eta$ —enhanced the number of metastatic sites (Figs 5B and 5E and Data Supplement) but not metastatic cells at death (Figs 5C and 5F). The number of metastatic sites decreased as the remaining tumor mass after surgery decreased (Fig 5H), likely as a result of a decreasing number of type-1 cells as the remaining primary tumor after resection decreased (Data Supplement). As expected, chemotherapies that decrease growth rates and increase death rates increase survival (Figs 5A and 5D and Figs 6A and 6B). Moreover, as the remaining primary tumor after resection decreased, the predicted survival in our model was extended, whereas the predicted survival was not dramatically enhanced when the remnant was smaller than 0.01 times the tumor volume at diagnosis (Figs 5G and 6C and Data

Supplement). Among all treatments options, the best predicted survival outcome was observed when patients experienced a large reduction of tumor growth rates—for instance, median survival was 113.4 months when  $\gamma = 0.1$  (Fig 6A). We also investigated the time of recurrence for patients who underwent surgical resection (Data Supplement). Of interest, the effect of chemotherapies that decrease growth rates was larger than that of those that increase death rates (Data Supplement). This observation might arise because the former more efficiently decreases the number of cell proliferation events than latter. Of note, the predictions of the effects on survival among different treatment options rely on modeling assumptions and the modeling definitions of clinical quantities, such as diagnosis and survival. It is beyond the scope of this work to translate the predicted effects of different treatment options into the clinical setting.

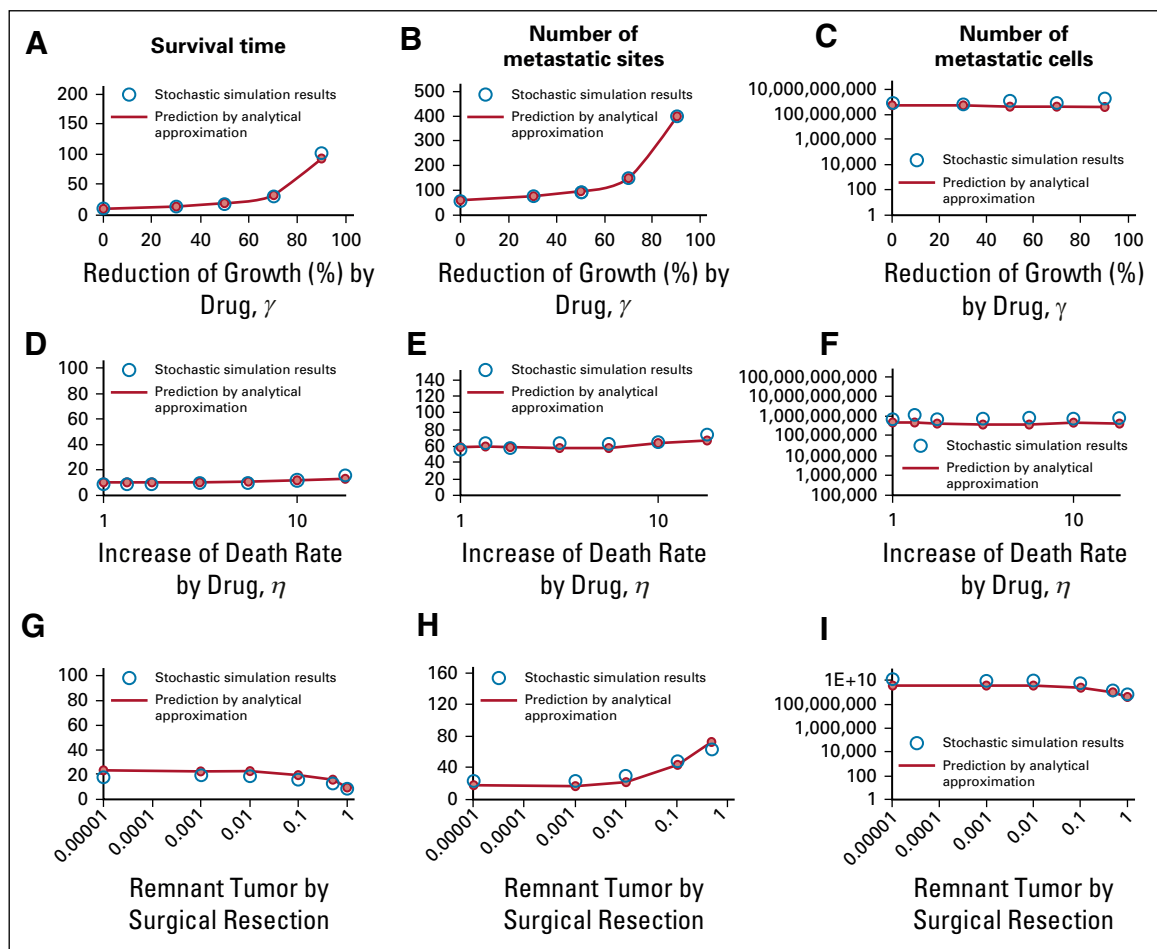


**FIG 5.** Three quantities at the time of death when chemotherapy is administered. Panels show the dependence of survival duration, the number of metastatic sites, and the number of metastatic cells on two kinds of chemotherapeutic effects: (A-C) chemotherapy, which reduces the growth rate of all tumor cells by  $\gamma$ ; (D-F) chemotherapy, which increases the death rate of all tumor cells by  $\eta$ ; and (G-I) surgical resection, which reduces the number of primary cells by  $(1-\epsilon)$ . The remnant fraction of a primary tumor after surgery is shown on the x-axis. The red curves indicate the predictions of the analytical approximation, Equations 8, 9, and 11, and the circles indicate the results of computer simulations. Parameters are  $r_0 = r_1 = 0.16$ ;  $r_2 = 0.58$ ;  $d_0 = d_1 = 0.0016$ ;  $d_2 = 0.0058$ ;  $M_{diag} = 5.3 \times 10^9$ ;  $M_{death} = 1.0 \times 10^{10}$ ;  $u = 6.31 \times 10^{-5}$ ;  $q = 6.31 \times 10^{-7}$ ;  $M_{carryP} = 1.3 \times 10^{10}$ ; and  $M_{carryM} \sim N(2.5, 5.3)$  cm.

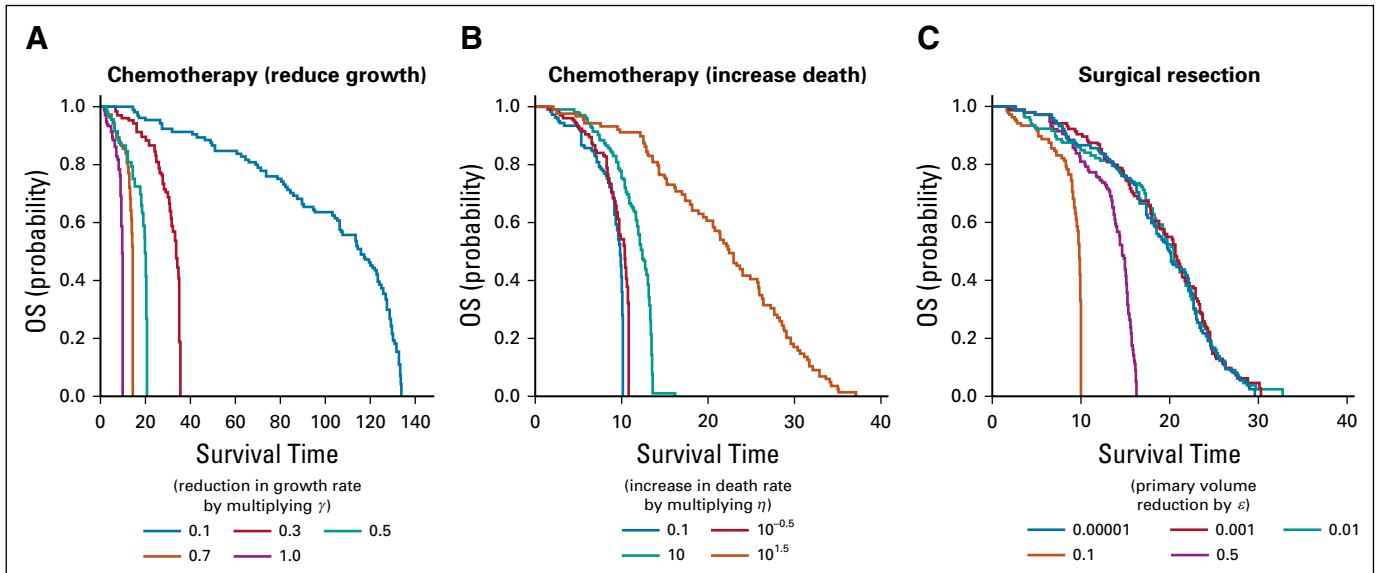


**FIG 6.** Kaplan-Meier analysis of overall survival (OS) in different treatment groups. The graphic shows the survival probability for the use of (A) chemotherapy, which reduces the growth rate of all tumor cells by  $\gamma$ ; (B) chemotherapy, which increases the death rate of all tumor cells by  $\eta$ ; and (C) surgical resection, which reduces the number of primary cells by  $1-\epsilon$ . We simulated the survival time of 100 patients with respect to each set of parameters. The values of parameters are the same as those described in Figure 5.

### Investigations of Intratumor Heterogeneity

To address the dynamics of intratumor heterogeneity in our pancreatic cancer progression model, we investigated an expanded model that incorporated heterogeneities in the growth kinetics of type-1 cells. Specifically, in this model, the growth rate of type-1 cells is a random variable drawn from a nondegenerate probability distribution. Whenever a type-1 cell is generated from a type-0 cell, its growth rate is chosen from a normal distribution whose mean was estimated from data obtained within the rapid pancreatic autopsy program<sup>19</sup> and different variances (Data Supplement). When analyzing this model, we found that the number of metastatic sites and cells as well as the number of type-1 cells did not change significantly when the variance of the type-1 growth rate distribution was small; however, these quantities became more and more different from the predictions of the original model when the variance of the growth rate distribution increased (Data Supplement). This observation arises because type-1 clones with high fitness may be selected in the primary site and preferably generate metastatic cells.

### DISCUSSION

Given the accumulating empirical evidence of a slowdown in tumor growth kinetics over time, such phenomena should be incorporated into mathematical models of metastasis formation.<sup>30-35</sup> In this work, we established a three-step logistic stochastic model of the evolution of metastases in pancreatic cancer. We derived analytical approximations

for the time from the initiation of tumorigenesis until diagnosis, the expected number of metastatic sites at a particular time, the total number of metastatic cells at a particular time, the number of primary tumor cells at a particular time during the clinical course of the disease, and survival depending on various treatment options for the specified modeling assumptions.

Our findings have several potential clinical implications. We observed that a decrease in the maximum size of the primary tumor—that is, the carrying capacity—increased the time from the initiation of tumorigenesis until diagnosis, the number of metastatic sites, and the number of metastatic cells (Figs 2F, 3F, and 4F). These results may explain the clinical observation that, at the time of death, 9% of patients in our pancreatic cancer autopsy cohort did not have a detectable primary tumor although they harbored multiple metastases.<sup>37</sup> Moreover, a recent study showed that 30% of patients were found to die of locally destructive disease in the autopsy program; 12% of patients had no metastases and an additional 18% had limited metastatic burden, contrary to the common belief that all patients with pancreatic cancer die of widely metastatic disease.<sup>37,40</sup> Our framework also describes these locally destructive cases: We found that an increase in the carrying capacity of the primary site led to fewer metastatic sites and metastatic cells (Figs 3F and 4F). Of importance, the natural course of pancreatic cancer in the context of this diversity of disease progression was not explained by previously used exponential growth models.<sup>19</sup> Of note, our *in silico* predictions

rely on the modeling assumptions. Clinical validation is necessary before making definite conclusions from model-based predictions.

Another interesting implication of our model pertains to studying the effects of the remaining fraction of the primary tumor after resection on survival. Complete tumor resection is a highly relevant prognostic factor for resectable pancreatic cancer.<sup>41,42</sup> A recent systematic review of four randomized controlled trials revealed that there was no difference in survival between R0—microscopic tumor clearance—and R1—microscopic residual tumor—resections.<sup>43</sup> Using our mathematical model, we investigated how different resection rates of the primary tumor influenced predicted patient survival (Fig 5G and Fig 6C). Of interest, we found that survival was not enhanced when the remnant was smaller than 0.01 times the tumor volume at diagnosis, which supports the results of the systematic review.<sup>43</sup> These results may indicate that metastatic cells that emerge before diagnosis contribute more to survival outcomes than do primary tumor cells. Among various relevant treatments, the most effective option to prolong both time until recurrence in post-surgical cases and survival was found to be one that reduces the growth rates of primary cells (Fig 6A and Data Supplement). These results indicate that chemotherapies that reduce primary growth rates may be effective in various clinical settings, such as in patients with metastatic disease or patients who received surgical resection of their primary site.

Apart from the logistic growth function, there also exist other alternative density-dependent tumor growth models, such as the Gompertz function. In both logistic and Gompertz functions, growth rates decrease as the total number reaches a certain level. Especially in the logistic function, the growth rate of a tumor cell population without competition can be explicitly defined by a parameter of net growth. As we have previously estimated the net growth rate of a pancreatic tumor cell population without competition using clinical data,<sup>19</sup> we adopted a logistic function for our model. We also assumed continuous dosing for chemotherapies. Evaluation of more realistic pulsed therapies by introducing time inhomogeneities of the rate parameters will be the topic of future investigations once pharmacokinetics/pharmacodynamics data become available.

In sum, our model can be used to predict the probability and time course of metastatic formation and the outcomes of treatment of pancreatic cancer. Our model might be applicable to other cancer types, provided that the model parameters can be identified using time series radiographic images from clinical samples. Using time series tumor volume data in the absence of treatments, we were able to determine growth kinetics of pancreatic cancer by comparing the goodness of fit of various growth models, which enabled us to estimate division and death rates of pancreatic cancer cells when analyzed by linear or nonlinear mixed-effects models. Our model may also be expanded to compare the efficacy of alternative treatment strategies in various scenarios.

## AFFILIATIONS

<sup>1</sup>Dana-Farber Cancer Institute, Boston, MA

<sup>2</sup>Harvard TH Chan School of Public Health, Boston, MA

<sup>3</sup>Harvard University, Cambridge, MA

<sup>4</sup>Medical College Hospital, Osaka, Japan

<sup>5</sup>Massachusetts General Hospital, Boston, MA

<sup>6</sup>Kyushu University, Fukuoka, Japan

<sup>7</sup>The Broad Institute of the Massachusetts Institute of Technology and Harvard, Cambridge, MA

<sup>8</sup>The Ludwig Center at Harvard, Boston, MA

**Provision of study materials or patients:** Kimiyo N. Yamamoto

**Collection and assembly of data:** Kimiyo N. Yamamoto, Akira Nakamura, Franziska Michor

**Data analysis and interpretation:** All authors

**Manuscript writing:** All authors

**Final approval of manuscript:** All authors

**Accountable for all aspects of the work:** All authors

## CORRESPONDING AUTHOR

Franziska Michor, PhD, Department of Data Sciences, Center for Cancer Evolution, Dana-Farber Cancer Institute, 450 Brookline Ave, Boston, MA 02215; e-mail: michor@jimmy.harvard.edu.

## AUTHOR CONTRIBUTIONS

**Conception and design:** Kimiyo N. Yamamoto, Akira Nakamura, Franziska Michor

## AUTHORS' DISCLOSURES OF POTENTIAL CONFLICTS OF INTEREST

The following represents disclosure information provided by authors of this manuscript. All relationships are considered compensated. Relationships are self-held unless noted. I = Immediate Family Member, Inst = My Institution. Relationships may not relate to the subject matter of this manuscript. For more information about ASCO's conflict of interest policy, please refer to [www.asco.org/rwc](http://www.asco.org/rwc) or [ascopubs.org/jco/site/ifc](http://ascopubs.org/jco/site/ifc).

**Hiroshi Haeno**

**Research Funding:** Boehringer Ingelheim

No other potential conflicts of interest were reported.

## REFERENCES

1. Siegel R, Naishadham D, Jemal A: Cancer statistics, 2012. *CA Cancer J Clin* 62:10-29, 2012
2. Hüsemann Y, Geigl JB, Schubert F, et al: Systemic spread is an early step in breast cancer. *Cancer Cell* 13:58-68, 2008
3. Fidler IJ: The pathogenesis of cancer metastasis: The 'seed and soil' hypothesis revisited. *Nat Rev Cancer* 3:453-458, 2003
4. Cao H, Xu E, Liu H, et al: Epithelial-mesenchymal transition in colorectal cancer metastasis: A system review. *Pathol Res Pract* 211:557-569, 2015

5. Battle E, Sancho E, Francí C, et al: The transcription factor snail is a repressor of E-cadherin gene expression in epithelial tumour cells. *Nat Cell Biol* 2:84-89, 2000
6. Comijn J, Berx G, Vermassen P, et al: The two-handed E box binding zinc finger protein SIP1 downregulates E-cadherin and induces invasion. *Mol Cell* 7:1267-1278, 2001
7. Yang J, Mani SA, Donaher JL, et al: Twist, a master regulator of morphogenesis, plays an essential role in tumor metastasis. *Cell* 117:927-939, 2004
8. Gumireddy K, Li A, Gimotty PA, et al: KLF17 is a negative regulator of epithelial-mesenchymal transition and metastasis in breast cancer. *Nat Cell Biol* 11:1297-1304, 2009
9. Murugaesu N, Iravani M, van Weverwijk A, et al: An in vivo functional screen identifies ST6GalNAc2 sialyltransferase as a breast cancer metastasis suppressor. *Cancer Discov* 4:304-317, 2014
10. Thiery JP, Acloque H, Huang RY, et al: Epithelial-mesenchymal transitions in development and disease. *Cell* 139:871-890, 2009
11. Altrock PM, Liu LL, Michor F: The mathematics of cancer: Integrating quantitative models. *Nat Rev Cancer* 15:12:730, 2015
12. Anderson AR, Chaplain MA, Newman EL, et al: Mathematical modelling of tumour invasion and metastasis. *Comput Math Methods Med* 2:129-154, 2000
13. Bosl GJ, Geller NL, Cirrincione C, et al: Multivariate analysis of prognostic variables in patients with metastatic testicular cancer. *Cancer Res* 43:3403-3407, 1983
14. Panetta JC: A mathematical model of periodically pulsed chemotherapy: Tumor recurrence and metastasis in a competitive environment. *Bull Math Biol* 58:425-447, 1996
15. Thames HD, Buchholz TA, Smith CD: Frequency of first metastatic events in breast cancer: Implications for sequencing of systemic and local-regional treatment. *J Clin Oncol* 17:2649-2658, 1999
16. Wodarz D, Anton-Culver H: Dynamical interactions between multiple cancers. *Cell Cycle* 4:764-771, 2005
17. Michor F, Nowak MA, Iwasa Y: Stochastic dynamics of metastasis formation. *J Theor Biol* 240:521-530, 2006
18. Dingli D, Michor F, Antal T, et al: The emergence of tumor metastases. *Cancer Biol Ther* 6:383-390, 2007
19. Haeno H, Gonen M, Davis MB, et al: Computational modeling of pancreatic cancer reveals kinetics of metastasis suggesting optimum treatment strategies. *Cell* 148:362-375, 2012
20. Yamamoto KN, Nakamura A, Haeno H: The evolution of tumor metastasis during clonal expansion with alterations in metastasis driver genes. *Sci Rep* 5:15886, 2015
21. Yamamoto KN, Hirota K, Takeda S, et al: Evolution of pre-existing versus acquired resistance to platinum drugs and PARP inhibitors in BRCA-associated cancers. *PLoS One* 9:e105724, 2014
22. Anderson AR: A hybrid mathematical model of solid tumour invasion: The importance of cell adhesion. *Math Med Biol* 22:163-186, 2005
23. Jain RK, Tong RT, Munn LL: Effect of vascular normalization by antiangiogenic therapy on interstitial hypertension, peritumor edema, and lymphatic metastasis: Insights from a mathematical model. *Cancer Res* 67:2729-2735, 2007
24. Scott JG, Fletcher AG, Maini PK, et al: A filter-flow perspective of haematogenous metastasis offers a non-genetic paradigm for personalised cancer therapy. *Eur J Cancer* 50:3068-3075, 2014
25. Newton PK, Mason J, Bethel K, et al: A stochastic Markov chain model to describe lung cancer growth and metastasis. *PLoS One* 7:e34637, 2012
26. Newton PK, Mason J, Bethel K, et al: Spreaders and sponges define metastasis in lung cancer: A Markov chain Monte Carlo mathematical model. *Cancer Res* 73:2760-2769, 2013
27. Collins VP, Loeffler RK, Tivey H: Observations on growth rates of human tumors. *Am J Roentgenol Radium Ther Nucl Med* 76:988-1000, 1956
28. Steel GG: *Growth Kinetics of Tumors: Cell Population Kinetics in Relation to the Growth and Treatment of Cancer*. Oxford, United Kingdom, Clarendon Press, 1977
29. Hart D, Shochat E, Agur Z: The growth law of primary breast cancer as inferred from mammography screening trials data. *Br J Cancer* 78:382-387, 1998
30. Laird AK: Dynamics of tumour growth: Comparison of growth rates and extrapolation of growth curve to one cell. *Br J Cancer* 19:278-291, 1965
31. Steel GG, Lamerton LF: The growth rate of human tumours. *Br J Cancer* 20:74-86, 1966
32. Spratt JA, von Fournier D, Spratt JS, et al: Decelerating growth and human breast cancer. *Cancer* 71:2013-2019, 1993
33. Akanuma A: Parameter analysis of Gompertzian function growth model in clinical tumors. *Eur J Cancer* 14:681-688, 1978
34. Norton L, Simon R: Growth curve of an experimental solid tumor following radiotherapy. *J Natl Cancer Inst* 58:1735-1741, 1977
35. Benzekry S, Lamont C, Beheshti A, et al: Classical mathematical models for description and prediction of experimental tumor growth. *PLOS Comput Biol* 10:e1003800, 2014
36. Vaidya VG, Alexandro FJ Jr: Evaluation of some mathematical models for tumor growth. *Int J Biomed Comput* 13:19-36, 1982
37. Iacobuzio-Donahue CA, Fu B, Yachida S, et al: DPC4 gene status of the primary carcinoma correlates with patterns of failure in patients with pancreatic cancer. *J Clin Oncol* 27:1806-1813, 2009
38. Kadaba R, Birke H, Wang J, et al: Imbalance of desmoplastic stromal cell numbers drives aggressive cancer processes. *J Pathol* 230:107-117, 2013
39. Iwasa Y, Nowak MA, Michor F: Evolution of resistance during clonal expansion. *Genetics* 172:2557-2566, 2006
40. Yamamoto KN, Yachida S, Nakamura A, et al: Personalized management of pancreatic ductal adenocarcinoma patients through computational modeling. *Cancer Res* 77:3325-3335, 2017
41. Sohn TA, Yeo CJ, Cameron JL, et al: Resected adenocarcinoma of the pancreas-616 patients: Results, outcomes, and prognostic indicators. *J Gastrointest Surg* 4:567-579, 2000
42. Wagner M, Redaelli C, Lietz M, et al: Curative resection is the single most important factor determining outcome in patients with pancreatic adenocarcinoma. *Br J Surg* 91:586-594, 2004
43. Butturini G, Stocken DD, Wentz MN, et al: Influence of resection margins and treatment on survival in patients with pancreatic cancer: Meta-analysis of randomized controlled trials. *Arch Surg* 143:75-83, discussion 83, 2008

